Contribution from the Corporate Research Science Laboratories,
Exxon Research and Engineering Company, Annandale, New Jersey 08801

Electronic Structure and Bonding in Heterometallic Cubane-Type Clusters Having an $Mo_2M'_2S_4$ Core (M' = Fe, Co, Ni)

Suzanne Harris

Received April 3, 1987

The results of molecular orbital calculations are reported for $Mo_2Co_2S_4(dtc)_2(CH_3CN)_2(CO)_2$, $Mo_2Ni_2S_4(Cp)_2(CO)_2$, and $Mo_2Fe_2S_4(Cp)_2(CO)_4$. Each metal in these clusters can be viewed as part of an octahedral, tetrahedral, or square-pyramidal MS_3L_x fragment. The electronic structure and, in particular, the formation of metal-metal bonds in the clusters are influenced by the bonding within these fragments. Metal-metal bonds are formed between metal t_{2g}- or t_2-like fragment orbitals, while metal e_g- or e-like fragment orbitals do not take part in the metal-metal bonding. The ligand environment (both the ligand geometry and the nature of the ligands) of each metal has a strong influence on the relative energies of these t_{2g}-like and e_g-like orbitals and thus has a strong influence on the energies of the bonding, antibonding, and nonbonding cluster orbitals. The position of the nonbonding orbitals determines how many "metal" electrons the cluster can accommodate without the loss of metal-metal bonds. The charge distributions in the clusters are very similar, and the relative sizes of the metal-metal overlap populations indicate that the strength of the metal-metal bonds decreases in the order Mo-Mo > Mo-M' > M'-M'. Because of the weak interactions between the 3d metals, the lowest energy metal-metal antibonding orbital is antibonding between the 3d metals. As a result, the bond between the 3d metals is the first one affected by the occupation of an antibonding orbital.

Introduction

Homometallic cubane-type clusters having a core of the general formula M_4S_4 have been the subject not only of numerous experimental studies but also of various theoretical studies. The theoretical attempts to understand the electronic structure and properties of these clusters have ranged from qualitative and approximate molecular orbital treatments[1-7] to more exact spin- and space-unrestricted Xα calculations.[8,9] Most of these theoretical treatments have employed a molecular orbital approach to describe the electronic structure of the various clusters. Particularly noteworthy among the molecular orbital descriptions of the M_4S_4 clusters is the work of Dahl and co-workers.[3] By considering the symmetry of the clusters and the cluster orbitals, this group developed a qualitative molecular orbital picture that provides a very useful systematic description of the bonding in many of the homometallic M_4S_4 clusters. Although a closed-shell molecular orbital approach can provide an adequate description of the bonding for many of the M_4S_4 clusters, a complete picture of the electronic structure of some of these clusters is much more difficult to obtain. Among the most difficult clusters to describe are those in which each Fe in an $[Fe_4S_4]^{n+}$ core is also bound to one other π-donor ligand. These clusters can be viewed as containing weakly interacting high-spin tetrahedral Fe centers, and a closed-shell molecular orbital picture cannot describe the spin couplings and resulting paramagnetic spin states. The difficulty in adequately describing these interactions was discussed by Aizman and Case[8] and Noodleman et al.[9] in a series of papers describing the results of spin- and space-unrestricted Xα calculations for model clusters having the $[Fe_4S_4]^{n+}$ core. It is clear that the complete picture of the electronic structure of these clusters is quite complex. Even for the Fe_4S_4 clusters, however, molecular orbital schemes such as those of Dahl et al. provide a qualitative picture that allows a comparison between the general bonding scheme in these clusters and that in other M_4S_4 clusters.

Although a number of heterometallic $M_2M'_2S_4$[10-15] and $M_3M'S_4$[16-20] clusters have now been synthesized, no qualitative molecular orbital picture has been developed to describe the bonding in these clusters. In fact, the theoretical attempts at understanding the electronic structure of these systems are limited. The electronic structure of the model cluster $MoFe_3S_4(SH)_6^{3-}$ has been investigated by unrestricted Xα calculations.[21] Since this cluster falls into the same category as the Fe_4S_4 clusters discussed above (a paramagnetic cluster in which several high-spin metal ions are weakly coupled together), however, the picture of the electronic structure that emerges from these calculations is quite complex. Fortunately, many of the heterometallic clusters that have been synthesized do not fall into this class. They are diamagnetic clusters for which closed-shell molecular orbital calculations should provide a useful description of the bonding. In this paper we describe the results of Fenske-Hall[22] molecular orbital calculations for three such heterometallic clusters—$Mo_2Co_2S_4(S_2CNEt_2)_2(CH_3CN)_2(CO)_2$,[14] $Mo_2Ni_2S_4(C_5H_4Me)_2(CO)_2$,[11] and $Mo_2Fe_2S_4(C_5Me_5)_2(CO)_4$.[15] Since this set of $Mo_2M'_2S_4$ cubanes includes clusters where M' is one of several 3d metals, it provides an opportunity to investigate how the cluster bonding is affected by substituting one 3d metal for another. Also, this group of clusters provides examples of various ligand coordination geometries about the different metals in the clusters. We will see that the formation of metal-metal bonds is strongly influenced by the ligand environment of each of the metals in these clusters. Taking into account this strong ligand influence on the metal orbitals makes it possible to view the metal-metal cluster bonding in a straightforward manner. By

(1) Guerts, P. J. M.; Gosselink, J. W.; Van der Avoird, A.; Baerends, E. J.; Snijders, J. G. *Chem. Phys.* **1980**, *46*, 133-148.
(2) Thompson, A. J. *J. Chem. Soc., Dalton Trans.* **1981**, 1180-1189.
(3) Chu, C. T.-W.; Lo, F. Y.-K.; Dahl, L. F. *J. Am. Chem. Soc.* **1982**, *104*, 3409-3422 and references therein.
(4) Bottomley, F.; Grein, F. *Inorg. Chem.* **1982**, *21*, 4170-4178.
(5) Sung, S.-S.; Glidewell, C.; Butler, A. R.; Hoffmann, R. *Inorg. Chem.* **1985**, *24*, 3856-3859.
(6) Muller, A.; Jostes, R.; Eltzner, W.; Nie, C.-S.; Diemann, E.; Bogge, H.; Zimmerman, M.; Dartmann, M.; Reinsch-Vogell, U.; Che, S.; Cyvin, S. J.; Cyvin, B. N. *Inorg. Chem.* **1985**, *24*, 2872-2884.
(7) Williams, P. D.; Curtis, M. D. *Inorg. Chem.* **1986**, *25*, 4562-4570.
(8) Aizman, A.; Case, D. A. *J. Am. Chem. Soc.* **1982**, *104*, 3269-3279.
(9) Noodleman, L.; Norman, J. G., Jr.; Osborne, J. H.; Aizman, A.; Case, D. A. *J. Am. Chem. Soc.* **1985**, *107*, 3418.
(10) Brunner, H.; Wachter, J. *J. Organomet. Chem.* **1982**, *240*, C41-C44.
(11) Curtis, M. D.; Williams, P. D. *Inorg. Chem.* **1983**, *22*, 2661-2662.
(12) Brunner, H.; Kauermann, H.; Wachter, J. *Angew. Chem., Int. Ed. Engl.* **1983**, *22*, 549-550.
(13) Rauchfuss, T. B.; Weatherill, T. D.; Wilson, S. R.; Zebrowski, J. P. *J. Am. Chem. Soc.* **1983**, *105*, 6508-6509.
(14) Halbert, T. R.; Cohen, S. A.; Stiefel, E. I. *Organometallics* **1985**, *4*, 1689-1690.
(15) Brunner, H.; Janietz, N.; Wachter, J.; Zahn, T.; Ziegler, M. L. *Angew. Chem., Int. Ed. Engl.* **1985**, *24*, 133-135.
(16) Pasynskii, A. A.; Eremenko, I. L.; Orazsakhatov, B.; Kalinnikov, V. T.; Aleksandraov, G. G.; Struchkov, Y. T. *J. Organomet. Chem.* **1981**, *214*, 367.
(17) Eremenko, I. L.; Pasynskii, A. A.; Orazsakhatov, B.; Ellert, O. G.; Novotortsev, V. M.; Kalinnikov, V. T.; Porai-Koshits, M. A.; Antsyshkina, A. S.; Dikareva, L. M.; Ostrikova, V. N. *Inorg. Chim. Acta* **1983**, *73*, 225-229.
(18) Averil, B. A. In *Structure and Bonding*; Springer-Verlag: Berlin, 1983; Vol. 53, pp 59-103.
(19) Palermo, R. E.; Singh, R.; Bashkin, J. K.; Holm, R. H. *J. Am. Chem. Soc.* **1984**, *106*, 2600-2612 and references therein.
(20) Shibahara, T.; Akashi, H.; Kuroya, H. *J. Am. Chem. Soc.* **1986**, *108*, 1342-1343.
(21) Cook, M.; Karplus, M. *J. Am. Chem. Soc.* **1985**, *107*, 257-259.
(22) Hall, M. B.; Fenske, R. F. *Inorg. Chem.* **1972**, *11*, 768-775.

0020-1669/87/1326-4278$01.50/0

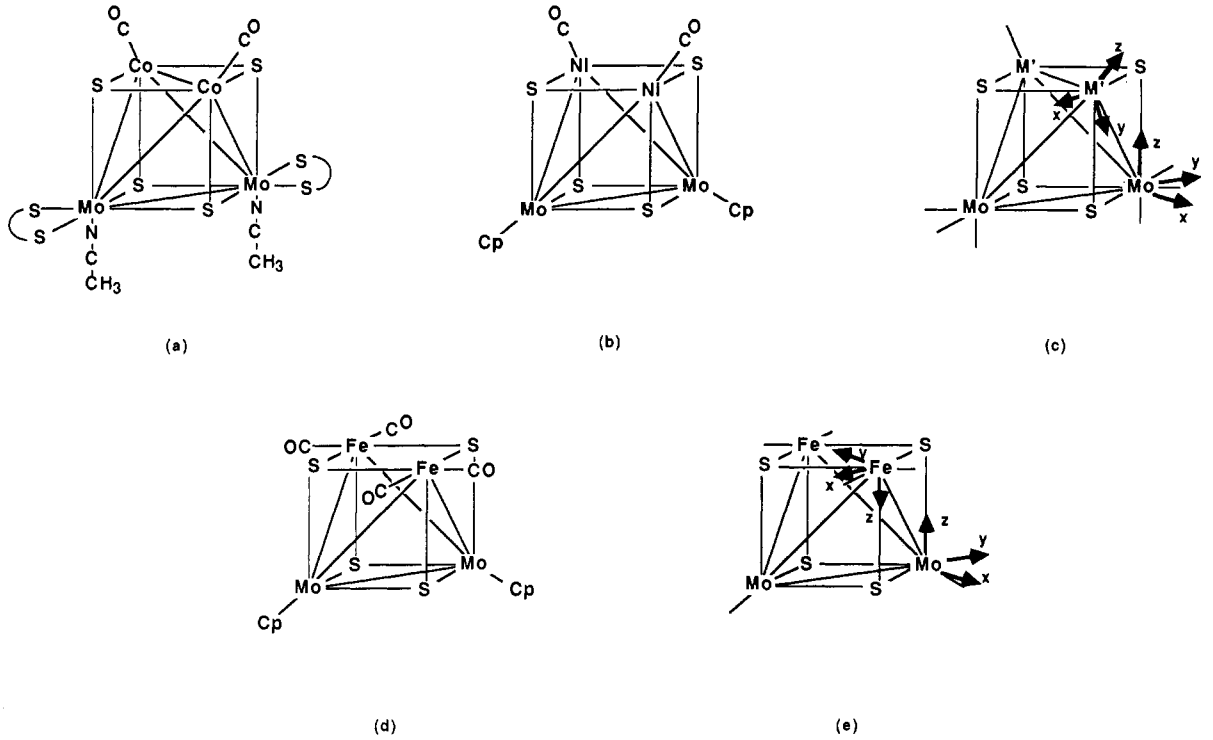

Figure 1. Schematic representations of the three cubane-type clusters and the orientations of the local metal coordinate systems used in the calculations. In $Mo_2Co_2S_4(dtc)_2(CH_3CN)_2(CO)_2$ (a) and $Mo_2Ni_2S_4(Cp)_2(CO)_2$ (b) each Mo lies in an octahedral environment and each Co or Ni lies in a tetrahedral environment. In these clusters the coordinate system on each metal is oriented as indicated in (c). In $Mo_2Fe_2S_4(Cp)_2(CO)_4$ (d) each Fe lies in a square-pyramidal environment. The orientations of the local coordinate systems for this cluster are indicated in (e).

considering the local environment and symmetry of each metal in a heterometallic $M_2M'_2S_4$ cluster, we can begin to develop a qualitative bonding picture for the heterometallic cubanes.

Calculational Details

All of the results described below for the heterometallic cubanes were obtained from Fenske–Hall molecular orbital calculations.[22] Calculations were carried out for $Mo_2Co_2S_4(S_2CNEt_2)_2(CH_3CN)_2(CO)_2$,[14] $Mo_2S_4(S_2CNEt_2)_2$,[23] $Mo_2Ni_2S_4(C_5H_4Me)_2(CO)_2$,[11] and $Mo_2Fe_2S_4(C_5Me_5)_2(CO)_4$,[15] all of whose structures have been determined. Atomic positions for these clusters were idealized to C_{2v} symmetries from the known structures. The ethyl groups in the $(S_2CNEt_2)^-$ ligands in the $Mo_2Co_2S_4$ cluster and in $MoS_4(S_2CNEt_2)_2$ were replaced with H's, and the $(C_5Me_5)^-$ groups in the $Mo_2Co_2S_4$ cluster and $(C_5H_4Me)^-$ groups in the $Mo_2Ni_2S_4$ cluster were replaced with $(C_5H_5)^-$ groups. Thus calculations were actually carried out for $Mo_2Co_2S_4(dtc)_2(CH_3CN)_2(CO)_2$, $Mo_2S_4(dtc)_2$, $Mo_2Ni_2S_4(Cp)_2(CO)_2$, and $Mo_2Fe_2S_4(Cp)_2(CO)_4$. The 1s through *n*d functions for Fe, Co, Ni, and Mo were taken from Richardson et al.,[24,25] while the $(n + 1)$s and $(n + 1)$p functions were chosen to have exponents of 2.0 for Fe, Co, and Ni and 2.2 for Mo. The carbon, nitrogen, oxygen, and sulfur functions were taken from the double-ζ functions of Clementi.[26] The valence p functions were retained as the double-ζ functions, while all other functions were reduced to single-ζ functions. An exponent of 1.2 was used for hydrogen. Mulliken population analyses were used to determine atomic charges and orbital populations.

Results and Discussion

The structures of $Mo_2Co_2S_4(dtc)_2(CH_3CN)_2(CO)_2$, $Mo_2Ni_2S_4(Cp)_2(CO)_2$, and $Mo_2Fe_2S_4(Cp)_2(CO)_4$ are illustrated (in a somewhat idealized form) in Figure 1. The local coordinate systems used in the calculations are also shown in Figure 1. All three of the clusters are drawn to emphasize the familiar "thiocubane" core. This core is characterized by two interpenetrating tetrahedra—a smaller one consisting of four metal atoms and a larger one consisting of four sulfur atoms. Each sulfur atom triply bridges three metal atoms. Each metal atom is also coordinated by one or more other ligands. In $Mo_2Co_2S_4(dtc)_2(CH_3CN)_2(CO)_2$, the metal–metal distances[14] are in a range is consistent with bonds between all of the metals. In $Mo_2Ni_2S_4(Cp)_2(CO)_2$ and $Mo_2Fe_2S_4(Cp)_2(CO)_4$ long Ni–Ni and Fe–Fe distances[11,15] of 2.96 and 3.33 Å, respectively, preclude a metal–metal bond between the 3d metals, but the other metal–metal distances are consistent with metal–metal bonds. Thus, the metal tetrahedron in $Mo_2Co_2S_4(dtc)_2(CH_3CN)_2(CO)_2$ is distorted by the presence of two different metals but is completely metal–metal bonded. The metal tetrahedra in $Mo_2Ni_2S_4(Cp)_2(CO)_2$ and $Mo_2Fe_2S_4(Cp)_2(CO)_4$ are further distorted by the long nonbonding distances between the 3d metals and can be described as having only five metal–metal bonds.

In order to describe the bonding in these cubanes, it is useful to think of the clusters in terms of various components or fragments and to then describe the metal–metal bond formation in terms of orbitals associated with each of these fragments. Such an approach has proved extremely useful for describing the bonding in many organometallic clusters (particularly metal carbonyl clusters)[27-29] where the stronger metal–ligand interactions and the weaker metal–metal interactions can be viewed separately. In metal carbonyl clusters, for example, it is possible (for the theoretician) to build a cluster from several $M(CO)_x$ fragments. The metal–metal bonds in the cluster can then be described in terms of metal-based fragment orbitals. The number, nature, and relative energy of these fragment orbitals are determined largely by the number and geometry of the ligands in the $M(CO)_x$ fragment. Each fragment can usually be viewed as some part of an octahedron, and the fragment metal orbitals that are available for cluster formation can be related to the t_{2g} and e_g orbitals in an octahedral complex. Upon formation of the cluster, the lower energy t_{2g}-like orbitals remain nonbonding between the metals, while the higher energy e_g-like orbitals on each fragment are

(23) Hunecke, J. T.; Enemark, J. H. *Inorg. Chem.* **1978**, *17*, 3698–3699.
(24) Richardson, J. W.; Nieuwpoort, W. C.; Powell, R. R.; Edgell, W. F. *J. Chem. Phys.* **1962**, *36*, 1057–1061.
(25) Richardson, J. W.; Blackman, M. J.; Ranochak, J. E. *J. Chem. Phys.* **1973**, *58*, 3010–3017.
(26) Clementi, E. *J. Chem. Phys.* **1964**, *40*, 1944–1945.
(27) Elian, M.; Hoffmann, R. *Inorg. Chem.* **1975**, *14*, 1058–1076.
(28) Hoffmann, R. *Science (Washington, D.C.)* **1981**, *211*, 995.
(29) Albright, T. E.; Burdett, J. K.; Whangbo, M.-H. *Orbital Interactions in Chemistry*; Wiley: New York, 1985.

utilized for the formation of metal–metal bonds. The spatial orientation of the e_g-like fragment orbitals is such that formation of the metal–metal bonds tends to complete the octahedral coordination about each metal.

Although it is not quite straightforward, it is also very useful to view the metal–metal bonding in the $M_2M'_2S_4$ clusters in terms of fragment orbitals. For the description of the electronic structure in these clusters, there are three sets of bonds that need to be considered. These are the metal–ligand bonds, the metal–sulfur bonds within the $M_2M'_2S_4$ core, and the metal–metal bonds. The interactions of the metals with both the ligands and the core sulfurs are stronger than the interactions between the metals. Thus, in the discussions that follow, all of the metal–ligand and metal–sulfur interactions will be grouped together (we will call them, collectively, metal–ligand interactions) and viewed separately from the metal–metal interactions. In this way we can consider fragments within the clusters and describe how the bonding within these fragments influences the formation of metal–metal bonds within the larger clusters. The complication here, compared to the case of metal carbonyl clusters, lies in the fact that the $M_2M'_2S_4$ clusters cannot be simply assembled from fragments. Instead, it is necessary to look at each metal and its ligand environment within the cluster, determine how this environment influences the metal-based orbitals, and then follow how these metal-based orbitals are used for the formation of metal–metal bonds. For example, if we ignore the metal–metal bonds in $Mo_2Co_2S_4(dtc)_2(CH_3CN)_2(CO)_2$, each Mo lies within the pseudooctahedral environment defined by the three core sulfurs, the bidentate dtc ligand, and the acetonitrile ligand. Each Co lies within the pseudotetrahedral environment defined by three sulfurs and the carbonyl ligand. Thus, from the point of view of the metals, there are four fragments in each cluster, two "octahedral" $MoS_3(dtc)_2(CH_3CN)$ fragments and two "tetrahedral" $CoS_3(CO)$ fragments. The other clusters can be described in a similar way. In $Mo_2Ni_2S_4(Cp)_2(CO)_2$, considering each Cp ligand as occupying three coordination sites on Mo, there are two "octahedral" MoS_3Cp fragments and two "tetrahedral" $CoS_3(CO)$ fragments. In $Mo_2Fe_2S_4(Cp)_2(CO)_4$ there are once again two "octahedral" MoS_3Cp fragments, but the disposition of the ligands around each Fe is such that there are now two "square-pyramindal" $FeS_3(CO)_2$ fragments. The strongest interactions in each cluster occur within these fragments, and thus for each cluster there will be numerous low-energy molecular orbitals associated with ligand and metal-ligand bonds. Once these bonds have been separated, the remaining metal–based "fragment" orbitals can be considered. It is these metal orbitals that combine to form the metal–metal bonds and the higher energy "frontier" orbitals in the clusters. (It is important to note here that since the fragment orbitals which we call "metal based" are for the most part the antibonding counterparts of the metal–ligand bonding orbitals, they do contain some ligand character. They are primarily metal in character, however, and thus may reasonably be described as metal-based orbitals.) Just as in the metal carbonyl clusters, these "fragment" metal orbitals fall into t_{2g}- and e_g-type groups (t_2 and e groups in the tetrahedral fragments). Unlike the case of metal carbonyl clusters, however, it is the t_{2g}-type metal orbitals that are used to form metal–metal bonds, while the e_g-type orbitals remain nonbonding with respect to metal–metal bonds. We will see below that the energies of these groups of metal-based fragment orbitals and thus the metal-based cluster orbitals are strongly influenced by the number, type, and geometry of the ligands in each MS_3L_x fragment. We will also see that, by taking into account the effect of the metal–ligand bonding on the energies of the orbitals used for metal–metal bonding, we can view the metal–metal bonding in these quite complex clusters in a fairly straightforward manner.

$Mo_2Co_2S_4(dtc)_2(CH_3CN)_2(CO)_2$. The calculated energy level diagram for $Mo_2Co_2S_4(dtc)_2(CH_3CN)_2(CO)_2$ is shown in Figure 2. Only the higher energy metal-based levels are shown. The numerous lower energy orbitals that correspond to the ligand and metal–ligand bonding orbitals are not included in the diagram because the following discussuion will focus primarily on metal–metal bonding. Also shown in Figure 2 are the calculated

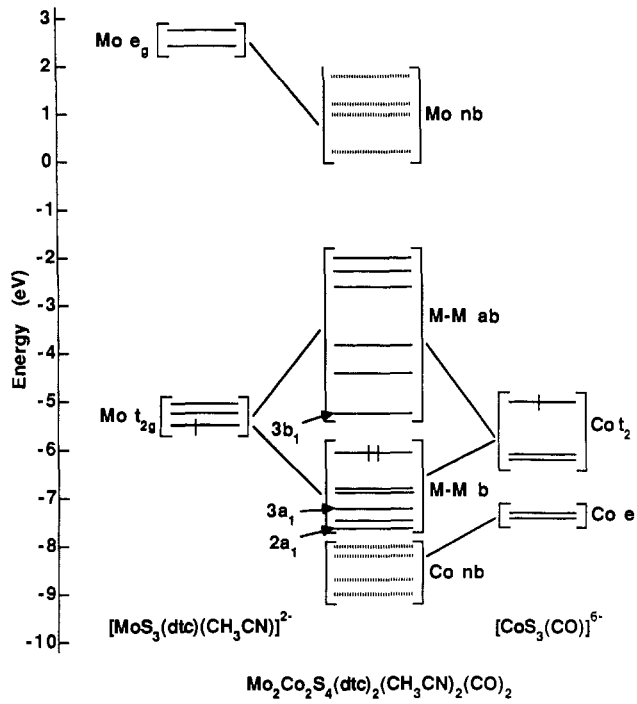

Figure 2. Calculated energy level diagrams for $Mo_2Co_2S_4(dtc)_2(CH_3CN)_2(CO)_2$ and for the $[MoS_3(dtc)(CH_3CN)]^{2-}$ and $[CoS_3(CO)]^{6-}$ fragments.

energies of the metal-based orbitals of the $[MoS_3(dtc)(CH_3CN)]^{2-}$ and $[CoS_3(CO)]^{6-}$ fragments. (The charges on the fragments are chosen to give the metal the same formal oxidation state it has in the overall cluster.) As was described above, each Mo can be viewed as having a pseudooctahedral environment, while each Co lies in a pseudotetrahedral environment. The effects of these environments are clearly recognizable for the two different fragments. The nearly octahedral environment of the molybdenums is reflected by sets of three and two orbitals that, although not degenerate, lie very close together in energy and correspond to the (d_{xz}, d_{yz}, $d_{x^2-y^2}$) and (d_{z^2}, d_{xy}) sets. (See Figure 1 for definition of the local coordinate system.) These two sets have been labeled as t_{2g} and e_g to emphasize the nearly octahedral environment around each Mo. The nearly tetrahedral environment of the cobalts is also reflected in the groupings of two and three orbitals, which once again are not degenerate but lie close enough in energy to be grouped together. These groups correspond, according to the local coordinate system shown in Figure 1, to the (d_{xz}, d_{yz}) and (d_{xy}, $d_{x^2-y^2}$, d_{z^2}) sets of orbitals. The two groups are labeled as e and t_2 to emphasize the nearly tetrahedral environment around each Co. (Note that actually groupings of two, two, and one levels are evident from the energy level diagram. These groupings reflect that the fragment actually has nearly C_{3v} symmetry. In this point group the three groups of orbitals would be labeled as e, e, and a_1, where the higher energy a_1 orbital corresponds to the d_{z^2} orbital. We will continue to describe this as a tetrahedral fragment, however, since the tetrahedral field splitting of the Co orbitals is important for the discussion that follows.) It is also informative to compare the relative energies of the fragment orbitals. The energy of the molybdenum-based orbitals is higher than that of the cobalt-based orbitals, and the splitting of the molybdenum-based orbitals in their octahedral environment is considerably larger than the splitting of the cobalt orbitals in their tetrahedral environment. The tetrahedral splitting of the Co orbitals is influenced by the presence of the π-acceptor CO ligand. This π-acceptor ligand stabilizes the e set of orbitals, resulting in a larger tetrahedral splitting than we might observe if all four of the ligands were π donors. The fragment-orbital parentage of the various groups of cluster orbitals is indicated by lines connecting the sets of cluster and fragment orbitals.

An examination of the level diagram for the total $Mo_2Co_2S_4$ cluster shows that the metal-based cluster orbitals lie in several

distinct groups. The occupied orbitals consist of a group of four lower energy orbitals that are cobalt based and nonbonding (with respect to metal–metal bonds) and another group of six orbitals that are the bonding combinations of the t_{2g} and t_2 orbitals on the octahedral Mo and tetrahedral Co fragments. The unoccupied orbitals consist of the six antibonding combinations of the t_{2g} and t_2 fragment orbitals and four molybdenum-based orbitals that are nonbonding between the metals. There is some mixing between the two e sets of orbitals on the tetrahedral fragments in the formation of the cluster, but the major fragment-orbital parentage of the sets of cluster orbitals is as indicated in the diagram. Thus four nonbonding and six bonding levels of primarily metal character are occupied by the twenty available electrons. (When we count the metal oxidations states as Co^0 and Mo^{5+}, each Co contributes 9 electrons and each Mo contributes 1 electron to the cluster, giving a total of 20 electrons available to occupy the metal-based cluster orbitals.) The occupation of all six metal–metal bonding orbitals and none of the antibonding orbitals is consistent with the completely metal–metal-bonded structure.

It is important to recognize which metal orbitals are used for metal–metal bonding and how the energies and orderings of these metal orbitals are influenced by the number and nature of coordinating ligands. As noted earlier, metal–metal bonds in metal carbonyl clusters are generally formed between the e_g-like orbitals associated with the $M(CO)_x$ fragments. The formation of these bonds completes the octahedral coordination about each metal in the cluster. The t_{2g}-like orbitals are generally completely occupied and nonbonding. In the cubane-type clusters, each metal is coordinated to three core sulfurs and to one or more other ligands. In these clusters, the geometry around each metal is such that the t_{2g} or t_2 set of metal orbitals is used to form metal–metal bonds, while the e_g or e set of orbitals remains nonbonding. This can be seen quite easily for the octahedrally coordinated Mo in $Mo_2Co_2S_4(dtc)_2(CH_3CN)_2(CO)_2$. The e_g orbitals (d_{xy} and d_{z^2} in the local coordinate system shown in Figure 1) point directly at the six coordinating ligands and are not available for interaction with another metal. The t_{2g} orbitals ($d_{x^2-y^2}$, d_{xz}, and d_{yz} in the coordinate system in Figure 1) on each Mo, however, are oriented properly to form metal–metal bonds. Although it is not so transparent for the tetrahedral geometry of the Co in $Mo_2Co_2S_4(dtc)_2(CH_3CN)_2(CO)_2$, it is also the t_2-like orbitals that are used for metal–metal bond formation. Thus in $Mo_2Co_2S_4(dtc)_2(CH_3CN)_2(CO)_2$ the t_{2g} and t_2 orbitals combine to form a total of twelve cluster orbitals, six bonding and six antibonding with respect to metal–metal bonds, while the e_g and e orbitals remain nonbonding. Occupation of the six bonding orbitals accounts for the completely metal-bonded cluster. The relative energy of the four cobalt-based nonbonding orbitals is also very important, however, because the low energy of these four orbitals makes it possible for the cluster to accomodate eight more electrons than are necessary to form the metal–metal bonds without occupying any antibonding orbitals. The tetrahedral environment around the Co (and in particular the π-acceptor CO ligand) stabilizes the nonbonding e orbitals, thus making it possible to have a completely metal–metal bonded cluster with 20 "metal" electrons. A cluster of this geometry, in fact, *requires* 20 electrons in order to have a completely metal–metal bonded cluster. Fewer than 20 electrons would leave unoccupied bonding orbitals, while more than 20 electrons would necessitate occupation of antibonding levels. We will see below that this is the case for $Mo_2Ni_2S_4(Cp)_2(CO)_2$, which has the same geometry as $Mo_2Co_2S_4(dtc)_2(CH_3CN)_2(CO)_2$ but 22 "metal" electrons. To emphasize the importance of the local coordination geometry to the relative energies of the bonding, antibonding, and nonbonding cluster orbitals, we note that a different local coordination geometry that destabilizes the 3d metal nonbonding orbitals relative to the cluster bonding orbitals will require a different number of "metal" electrons for a completely metal–metal-bonded cluster. We will consider such a geometry when we discuss the bonding in $Mo_2Fe_2S_4(Cp)_2(CO)_4$.

Before we discuss the bonding in $Mo_2Ni_2S_4(Cp)_2(CO)_2$ and $Mo_2Fe_2S_4(Cp)_2(CO)_4$, however, there are several observations that can be made about the bonding in the $Mo_2Co_2S_4$ cluster. We have so far viewed the bonding in this cluster in terms of $[MoS_3(dtc)(CH_3CN)]^{2-}$ and $[CoS_3(CO)]^{6-}$ fragments and have ignored the fact that the cluster is actually prepared[14] by combining $Mo_2S_4(Et_2dtc)_2$ (**1**) with $Co_2(CO)_8$ in the presence of CH_3CN.

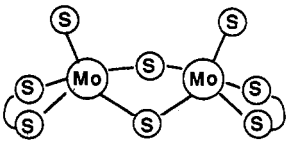

1

The $Mo_2Co_2S_4$ cube is formed by the addition of two Co(CO) units to the $Mo_2S_4(Et_2dtc)_2$ molecule, and the $Mo_2S_4(dtc)_2$ unit is easily identified in the $Mo_2Co_2S_4(dtc)_2(CH_3CN)_2(CO)_2$ cluster illustrated in Figure 1. In $Mo_2S_4(Et_2dtc)_2$, each Mo is five-coordinate and is part of a square pyramid, although the Mo's lie above the plane of the four sulfurs forming the base of the square pyramid.[23] Each molybdenum is formally Mo^{5+} and is thus a d^1 metal. When we use the same local coordinate system for the Mo's as that indicated in Figure 1, the Mo $d_{x^2-y^2}$ orbitals combine to form a σ-bonding orbital, which is occupied by the two metal electrons. When $Mo_2S_4(Et_2dtc)_2$ is incorporated into the cube, the $Mo_2S_4(Et_2dtc)_2$ molecule itself remains intact, but some changes do occur in its structure. In the cube, the dihedral angle between the bases of the two square pyramids opens by approximately 16° and the base of each square pyramid flattens so that the Mo lies nearer to the plane containing the four sulfurs. Also, the Mo–S_T bonds lengthen as the sulfurs form additional bonds to cobalt. Finally, the sixth coordination site on each Mo, which in the original $Mo_2S_4(Et_2dtc)_2$ molecule is vacant, is now occupied by an acetonitrile molecule. If we consider the $Mo_2S_4(Et_2dtc)_2$ entity within the larger cube, much of the orbital structure of this molecule is still identifiable within the cube. Some changes do occur, however, as the cube is formed, and these were followed by carrying out a series of calculations for several different structures.

Calculations were carried out for (1) $Mo_2S_4(dtc)_2$ in its normal configuration, (2) $Mo_2S_4(dtc)_2$ in the flattened configuration found in the cube, (3) $Mo_2Co_2S_4(dtc)_2(CO)_2$, the cube without the CH_3CN ligands, and finally (4) the complete $Mo_2Co_2S_4(dtc)_2(CH_3CN)_2(CO)_2$ cube. A comparison of the results of calculations 1 and 2 shows that flattening the $Mo_2S_4(dtc)_2$ entity weakens the interaction between the Mo's and terminal sulfurs (S_T in **1**) and clearly puts the terminal and bridging sulfurs into positon to bind more effectively to the cobalts. The results of calculation 3 are particularly interesting, because it has been suggested that the addition of the sixth ligand to each Mo in the cube brings the cluster electron count to 60 and thus may be necessary for the formation of the cube.[14] The orbital structure of the cube with no acetonitriles is shown in Figure 3, and it is apparent from a comparison with Figure 2 that the relative energies of the occupied oribtals in $Mo_2Co_2S_4(dtc)_2(CO)_2$ and $Mo_2Co_2S_4(dtc)_2(CH_3CN)_2(CO)_2$ are very similar. An examination of the characters of these orbitals shows that these also are nearly identical. As can be seen from the diagrams, the real difference lies in the unoccupied orbitals. In the octahedral environment in $Mo_2Co_2S_4(dtc)_2(CH_3CN)_2(CO)_2$, the Mo d_{z^2} orbital forms part of the nearly degenerate e_g set. In the square-pyramidal environment in $Mo_2Co_2S_4(dtc)_2(CO)_2$, however, the Mo d_{z^2} orbital lies considerably lower in energy than the d_{xy} orbital. As a result, the cluster orbitals that are formed from the Mo d_{z^2} orbitals are also lower in energy in $Mo_2Co_2S_4(dtc)_2(CO)_2$ than in $Mo_2Co_2S_4(dtc)_2(CH_3CN)_2(CO)_2$. This has a negligible effect on the overall electronic structure of the cluster itself, however, because the occupied orbitals are nearly identical in both clusters. Since the acetonitrile ligand is a weak σ donor and a very weak π acceptor, the orbitals that are necessary for metal–metal bond formation are minimally affected by the presence of this sixth ligand. Thus in this particular cluster, the coordination of the sixth ligand appears to be facilitated by the flattening of the Mo_2S_4

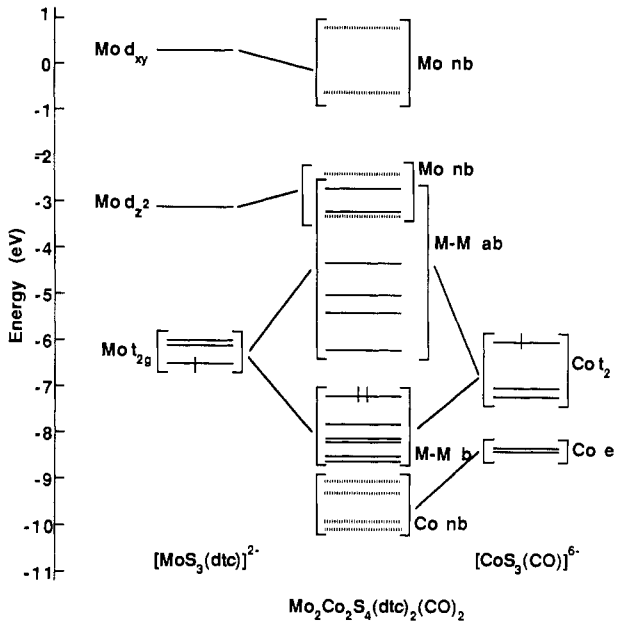

Figure 3. Calculated energy level diagrams for $Mo_2Co_2S_4(dtc)_2(CO)_2$ and for the $[MoS_3(dtc)]^{2-}$ and $[CoS_3(CO)]^{6-}$ fragments.

Table I. Metal d–d Overlap Populations

	Mo–Mo	Mo–M′	M′–M′
$Mo_2S_4(dtc)_2$	0.047		
$Mo_2Co_2S_4(dtc)_2(CH_3CN)_2(CO)_2$	0.058	0.019	0.005
$Mo_2Co_2S_4(dtc)_2(CO)_2$	0.058	0.016	0.004
$[Mo_2Co_2S_4(dtc)_2(CH_3CN)_2(CO)_2]^{2-}$	0.063	0.014	−0.006
$Mo_2Ni_2Cp_2S_4(CO)_2$	0.047	0.009	0.000
$Mo_2Fe_2S_4Cp_2(CO)_4$	0.063	0.014	−0.002

unit, which makes the Mo more accesible sterically, and the weakening of the Mo–S interactions upon formation of the cube. The presence of this sixth ligand is certainly not necessary, however, for the stability of the cube. In fact, it is probably preferable to say that coordination of the sixth ligand is not precluded by the electronic structure of the cube itself. The molecular and electronic structure of the cube makes it possible for a weakly bound ligand to occupy this sixth coordination site without perturbing the electronic structure of the overall cluster.

There are several other interesting features of the electron distributions in these clusters. The first of these is the relative strength of the 4d–4d, 4d–3d, annd 3d–3d metal–metal-bonding interactions. These strengths are reflected in the magnitude of the d–d overlap populations (Table I). In $Mo_2Co_2S_4(dtc)_2(CH_3CN)_2(CO)_2$, the 4d–4d overlap populations are about 3 times as large as the 4d–3d overlap populations, which in turn are about 4 times as large as the 3d–3d overlap populations. This reflects to some degree the orientation of the Co 3d orbitals in their tetrahedral environment, but the major reason for this trend is the difference in size of the 4d and 3d orbitals. At the metal–metal distances observed in these clusters, the orbital overlaps for the more compact first-row transition metals are considerably smaller than those for the larger second-row transition metals. Although the cobalts are certainly within bonding distance and can be considered to be bonded in the $Mo_2Co_2S_4$ cube, the interactions between the 3d metals are considerably weaker than those between the 4d metals. (This applies to interactions involving the s and p as well as the d orbitals.) Even the Mo–Mo and Mo–Co interactions are fairly weak so that much of the "glue" holding together the cluster is the large number of very delocalized molecular orbitals involving the sulfurs as well as the metals and not strong direct metal interactions. A comparison of the overlap populations in $Mo_2Co_2S_4(dtc)_2(CH_3CN)_2(CO)_2$ and $Mo_2Co_2S_4(dtc)_2(CO)_2$ shows that the presence of CH_3CN has little effect on these values. This is consistent with the discussion above.

Another quantity of interest is the calculated charge of each of the metal atoms. These charges are listed in Table II. The

Table II. Calculated Charges Based on Mulliken Populations

	Mo	M′
$Mo_2S_4(dtc)_2$	+1.339	
$Mo_2Co_2S_4(dtc)_2(CO)_2$	+1.114	+0.087
$Mo_2Co_2S_4(dtc)_2(CH_3CN)_2(CO)_2$	+1.139	+0.085
$[Mo_2Co_2S_4(dtc)_2(CH_3CN)_2(CO)_2]^{2-}$	+1.134	+0.099
$Mo_2Ni_2S_4Cp_2(CO)_2$	+1.345	−0.007
$Mo_2Fe_2S_4Cp_2(CO)_4$	+1.247	+0.181

calculated charge (based on Mulliken populations) of each Mo in $Mo_2S_4(dtc)_2$ is +1.34. Each Mo is of course formally Mo^{5+}, but this calculated value is in line with the covalency of the bonding and is about the value we might expect. The formation of the cube reduces this charge to +1.14, a fairly small effect. Since the Mo d_{xz} and d_{yz} orbitals are used in bonding to Co, the occupations of these orbitals increase upon formation of the Mo–Co bonds. At the same time, the occupations of the Mo orbitals involved in Mo–S bonds decrease. The net result is a small increase in the total 4d population and thus the small decrease in the calculated positive charge for Mo. As might be expected, the calculated charge for Co is closer to zero (+0.08) than that for Mo. It seems appropriate, on the basis of the calculated charges, to assign formal oxidation states of Mo^{5+} and Co^0 within the cube. The makeup of the Mo–Co bonding orbitals also supports this assignment. It is important to recognize, however, that in metal–sulfur clusters the relation between formal oxidation states and calculated charges is rather tenuous. For example, calculations on other heterometallic sulfur clusters show that a change in formal oxidation state of one of the metals results in a very small change in the calculated charge of the metal.[30] The many delocalized orbitals involving both metal and sulfur orbitals allow the effect of the addition or removal of an electron to be distributed over the entire cluster.

Finally, we consider how oxidation or reduction might change the structure of $Mo_2Co_2S_4(dtc)_2(CH_3CN)_2(CO)_2$. The characters of the occupied bonding orbitals and unoccupied antibonding orbitals are important in this regard. An examination of the bonding orbitals shows that only some of these orbitals are strongly metal–metal bonding. For example, the lowest energy bonding level ($2a_1$ in Figure 2) is strongly bonding between all four metal atoms. Likewise, the $3a_1$ orbital is localized and strongly bonding between the two Mo's. Several of the orbitals, however, are neither strongly localized nor strongly bonding. Thus, although we can formally equate the occupation of these six orbitals with six metal–metal bonds, the orbitals tend to be quite delocalized, and in general there is no one to one correspondence between a particular bond and a particular orbital. Removal of an electron from an orbital that is very strongly bonding or strongly localized between two atoms should have a very noticeable effect on the metal–metal bonds, while removal of an electron from a more delocalized or less strongly bonding orbital would have a much less measurable effect. In $Mo_2Co_2S_4(dtc)_2(CH_3CN)_2(CO)_2$, the higher energy occupied orbitals are delocalized and very weakly bonding, so we would expect that oxidation of the cluster would have only a small effect on the metal–metal distances. Although we make this observation for $Mo_2Co_2S_4(dtc)_2(CH_3CN)_2(CO)_2$, similar observations have previously been made for homometallic cubanes. It was observed, for example, that the oxidation of $Mo_4S_4(i\text{-}PrCp)_4$ to the 1+ and 2+ species has little effect on the structure of the Mo_4S_4 cube,[31] even though with just 12 electrons to occupy the six metal–metal bonding orbitals in the neutral cluster, oxidation removes an electron from one of these bonding levels. This suggests that oxidation results in the removal of an electron from an orbital that is not strongly bonding. A recent study of the electronic structure of several $M_4S_4Cp_4$ clusters[7] confirms that a number of the frontier orbitals in these clusters are very weakly bonding, so that removal of electrons from these levels would have very little effect on the metal–metal distances

(30) Bernholc, J.; Harris, S., unpublished results.
(31) Bandy, J. A.; Davies, C. E.; Green, J. C.; Green M. L. H.; Prout, K.; Rodgers, D. P. S. *J. Chem. Soc., Chem. Commun.* **1983**, 1395–1397.

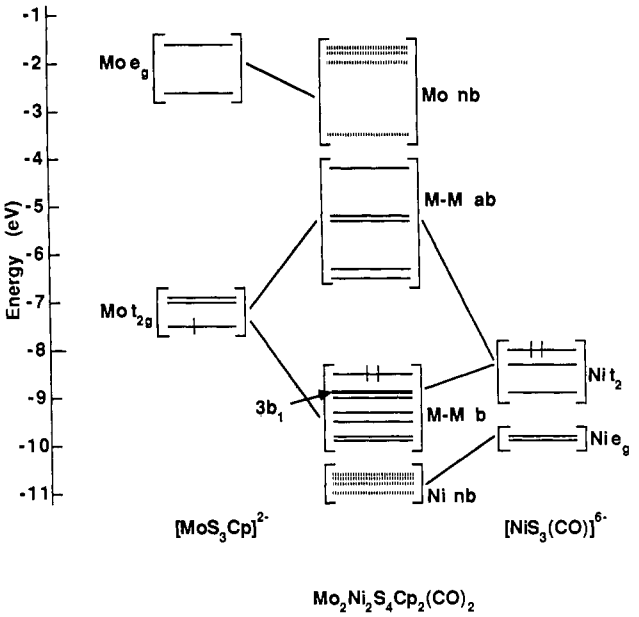

Figure 4. Calculated energy level diagrams for $Mo_2Ni_2S_4(Cp)_2(CO)_2$ and for the $[MoS_3(Cp)]^{2-}$ and $[NiS_3(CO)]^{6-}$ fragments.

in these clusters. Our calculations suggest that the same description applies to the heterometallic cubanes.

Reduction of $Mo_2Co_2S_4(dtc)_2(CH_3CN)_2(CO)_2$ will lead to occupation of an antibonding orbital, and the effect of occupying an antibonding level will again depend on the character of this orbital. Adding two electrons to the LUMO in $Mo_2Co_2S_4(dtc)_2(CH_3CN)_2(CO)_2$ is a particularly interesting excercise, because the addition of two electrons to the $Mo_2Co_2S_4$ core of $Mo_2Co_2S_4(dtc)_2(CH_3CN)_2(CO)_2$ makes it isoelectronic with the $Mo_2Ni_2S_4$ core of $Mo_2Ni_2S_4(Cp)_2(CO)_2$, which is the next cluster we wish to discuss. The LUMO ($3b_1$ in Figure 2) in $Mo_2Co_2S_4(dtc)_2(CH_3CN)_2(CO)_2$ is in fact antibonding between the two Co's. The fact that the LUMO in this cluster is antibonding between the two Co's is consistent with the observation that the weakest interactions in the cluster are those between the two Co's. Both the bonding and antibonding interactions are weak, so it is not surprising that the lowest energy antibonding orbital has a large Co contribution. When two electrons occupy the $3b_1$ orbital, the Co–Co d–d overlap population becomes −0.006 (Table I), indicating that the Co–Co interaction is now antibonding. The changes in the Mo–Mo and Mo–Co overlap populations are small, and any cluster distortion resulting from occupation of this orbital would be expected to push the two Co's apart. This is exactly the type of distortion observed in $Mo_2Ni_2S_4(Cp)_2(CO)_2$, where a long distance of 2.961 Å separates the two Ni's. This structure suggests that it is an orbital like the $3b_1$ orbital of $Mo_2Co_2S_4(dtc)_2(CH_3CN)_2(CO)_2$, which is occupied by the two additional electrons in $Mo_2Ni_2S_4(Cp)_2(CO)_2$. This will be discussed further below.

$Mo_2Ni_2S_4(Cp)_2(CO)_2$. The calculated energy level diagrams for $Mo_2Ni_2S_4(Cp)_2(CO)_2$ and for the $[MoS_3Cp]^{2-}$ and $[NiS_3(CO)]^{6-}$ fragments are shown in Figure 4. Once again, only the metal-based orbitals are shown in detail. When we look first at the fragments, the metal-based orbitals for both the octahedral and the tetrahedral fragments show the expected orderings. When the energies of the fragment orbitals in $Mo_2Ni_2S_4(Cp)_2(CO)_2$ are compared with the energies of the fragment orbitals in $Mo_2Co_2S_4(dtc)_2(CH_3CN)_2(CO)_2$ (Figure 2), however, two differences are apparent. The splitting between the t_{2g} and e_g orbitals is smaller in the $[MoS_3Cp]^{2-}$ fragment than in the $[MoS_3(dtc)(CH_3CN)]^{2-}$ fragment discussed above, and the Ni t_2 orbitals lie somewhat lower in energy relative to the Mo t_{2g} orbitals than do the corresponding Co t_2 orbitals. Neither of these differences, however, causes the overall cluster bonding in $Mo_2Ni_2S_4(Cp)_2(CO)_2$ to be substantially different from that observed in $Mo_2Co_2S_4(dtc)_2(CH_3CN)_2(CO)_2$. In fact, except for the absence of a bond between the Ni's, the bonding is remarkably similar. Once again, there are four groups of metal-based orbitals—the Ni nonbonding orbitals, the metal bonding orbitals, the metal antibonding orbitals, and the Mo nonbonding orbitals. As indicated in Figure 4, these orbitals are occupied through the set of orbitals labeled M—M bonding. As discussed above, the $Mo_2Ni_2S_4$ core must accommodate two more electrons than the corresponding $Mo_2Co_2S_4$ core. As a result, one antibonding orbital is occupied. The group of levels labeled M–M antibonding contains only five orbitals, while seven levels lie within the group of occupied orbitals labeled as M–M bonding. The occupied $3b_1$ orbital, which falls among these bonding levels, is actually antibonding between the Ni atoms and is the counterpart to the LUMO in $Mo_2Co_2S_4(dtc)_2(CH_3CN)_2(CO)_2$. The energy of the $3b_1$ orbital is lower in $Mo_2Ni_2S_4(Cp)_2(CO)_2$ because occupation of this orbital results in a distortion of the $Mo_2Ni_2S_4$ core, which pushes the two Ni's away from each other. At the resulting long Ni–Ni distance, the interaction between the Ni's is extremely weak and the $3b_1$ orbital drops in energy so that it lies within the group of metal–metal-bonding orbitals.

Table III. Examples of $M_2M'_2S_4$ Clusters with Octahedrally Coordinated M and Tetrahedrally Coordinated M'

	no. of "metal" electrons	ref
$Mo_2Co_2S_4(dtc)_2(CH_3CN)_2(CO)_2$	20	14
$M_2Co_2S_4(Me_5Cp)_2(CO)_2$ (M = Cr, Mo)	20	10
$Mo_2Fe_2S_4(Me_5Cp)_2(NO)_2$	20	12
$Mo_2Ni_2S_4(MeCp)_2(CO)_2$	22	11
$V_2Fe_2S_4(MeCp)_2(NO)_2$	18	13

The values of both the metal overlap populations in Table I and the calculated charges in Table II show that the electron distributions in $Mo_2Ni_2S_4(Cp)_2(Co)_2$ are very similar to those in $Mo_2Co_2S_4(dtc)_2(CH_3CN)_2(CO)_2$. The only significant difference is the absence of a Ni–Ni bond. Just as might be expected, the overlap populations show that there is no measurable bonding interaction between the two Ni's in $Mo_2Ni_2S_4(Cp)_2(CO)_2$. Other differences are very small. The Mo–Mo and Mo–Ni overlap populations are comparable to but slightly smaller than the corresponding quantities in $Mo_2Co_2S_4(dtc)_2(CH_3CN)_2(CO)_2$. The calculated charges indicate that Mo is slightly more positive and Ni slightly more negative in $Mo_2Ni_2S_4(Cp)_2(CO)_2$ than are Mo and Co in the $Mo_2Co_2S_4(dtc)_2(CH_3CN)_2(CO)_2$. It is difficult to make one to one comparisons, however, because these small differences may simply reflect the different coordinations around the Mo's in $Mo_2Co_2S_4(dtc)_2(CH_3CN)_2(CO)_2$ and $Mo_2Ni_2S_4(Cp)_2(CO)_2$. (We might expect, for example, Mo to be more positive when Cp replaces the dtc and CH_3CN ligands.) Thus, the similarities in the two clusters are far more obvious that any significant differences. We would expect that the bonding in other cubanes having the same structure should also be very similar. The formulas of several other clusters of this type are listed in Table III along with their electron counts. Where structures have been determined, these structures are consistent with the electron counts. It should be possible to synthesize other clusters that are combinations of different metals and/or ligands but have the appropriate electron count for a cluster with this structure.

$Mo_2Fe_2S_4(Cp)_2(CO)_4$. In this cluster each Mo is part of an octahedral MoS_3Cp fragment that is similar to that found in $Mo_2Ni_2S_4(Cp)_2(CO)_2$, while each Fe is part of a square-pyramidal $FeS_3(CO)_2$ fragment. The apical position of the square pyramid is occupied by a S, while two S's and the two C's of the CO ligands form the base of the square pyramid. Although the schematic diagram in Figure 1 suggests that the Fe lies in the same plane as the base of the square pyramid, it is actually displaced approximately 0.5 Å out of this plane toward the apical sulfur. We will return to this point later in the discussion. As was mentioned above, the Fe–Fe distance of 3.33 Å is sufficiently long to preclude an Fe–Fe bond, so the cluster can be described as a distorted cube with five metal–metal bonds.

The calculated energy level diagrams for $Mo_2Fe_2S_4(Cp)_2(CO)_4$ and for the $[MoS_3Cp]^{2-}$ and $[FeS_3(CO)_2]^{6-}$ fragments are shown

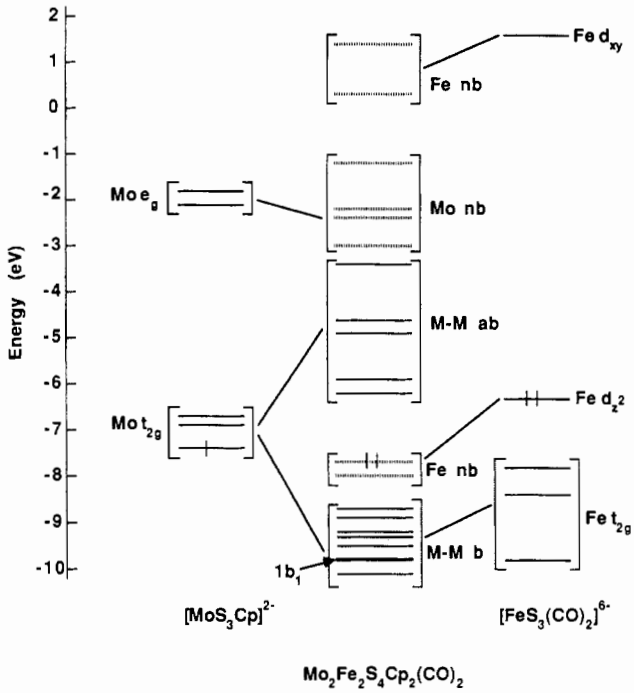

Figure 5. Calculated energy level diagrams for $Mo_2Fe_2S_4(Cp)_2(CO)_4$ and for the $[MoS_3(Cp)]^{2-}$ and $[FeS_3(CO)_2]^{6-}$ fragments.

in Figure 5. The Mo orbitals of the octahedral fragment are split into the familiar pattern of three lower energy t_{2g} orbitals and two higher energy e_g orbitals. The Fe orbitals in each square-pyramidal fragment are split so that three t_{2g}-like orbitals ($d_{x^2-y^2}$, d_{xz}, and d_{yz} in the local coordinate system shown in Figure 1) lie lowest in energy. The d_{xy} orbital lies highest in energy, while the d_{z^2} orbital lies at an intermediate energy. When we compare the relative energies of the orbitals in this square-pyramidal fragment to the relative energies of the orbitals in the square-pyramidal $[MoS_3(dtc)]^{2-}$ fragment in $Mo_2Co_2S_4(dtc)_2(CO)_2$ (Figure 3), two differences are immediately obvious. First, the energies of the three orbitals making up the t_{2g} set span a greater range in the $[FeS_3(CO)_2]^{6-}$ fragment than in the $[MoS_3(dtc)]^{2-}$ fragment. Second, and more importantly, the d_{z^2} orbital is stabilized to a much greater extent in the $[FeS_3(CO)_2]^{6-}$ fragment than in the $[MoS_3(dtc)]^{2-}$ fragment. This stabilization has important consequences for the metal–metal bonding in the cluster.

Looking next at the cluster orbitals, we see that there are two familar groups of bonding and antibonding orbitals resulting from combinations of the four sets of t_{2g} orbitals, but there are now three separate sets of nonbonding orbitals. Two sets of nonbonding orbitals (those corresponding to the two Fe d_{xy} orbitals and the four Mo e_g orbitals) lie at energies above the antibonding orbitals, but one set (that corresponding to the two Fe d_{z^2} orbitals) lies between the two groups of bonding and antibonding orbitals. Thus the 18 metal electrons (assigning formal oxidation states of Mo^{5+} and Fe^0) occupy six bonding orbitals, two nonbonding orbitals, and one antibonding orbital. As is indicated in Figure 5, the energy of this occupied antibonding orbital ($1b_1$) is low enough that it lies within the group of bonding levels. This position of the antibonding level, which is similar to that observed in $(C_5H_5)_2Mo_2Ni_2S_4(CO)_2$, results from the negligible interactions between the two Fe's at a distance of 3.33 Å.

The really interesting feature of the orbital structure of $Mo_2Fe_2S_4(Cp)_2(CO)_4$, however, is the low energy of the d_{z^2} orbital in relation to the other orbitals on the $[FeS_3(CO)_2]^{6-}$ fragment and the resulting low energy of the two nonbonding orbitals in the $Mo_2Fe_2S_4$ cluster. This allows the cluster to accommodate six electrons in excess of the number required to fill the bonding orbitals with a loss of only one metal–metal bond. We saw above when we compared $Mo_2Co_2S_4(dtc)_2(CH_3CN)_2(CO)_2$ with $Mo_2Co_2S_4(dtc)_2(CO)_2$ that although the change from octahedral to square-pyramidal coordination about the Mo resulted in the stabilization of the d_{z^2} orbitals, these orbitals were not sufficiently stabilized to be occupied in the $Mo_2Co_2S_4$ cluster. Why is the corresponding Fe d_{z^2} orbital so much more stabilized?

To understand the relative energies of the orbitals on the $[FeS_3(CO)_2]^{6-}$ fragment, it is necessary to look at the structure of the fragment. As mentioned above, the Fe atom lies about 0.5 Å out of the basal plane of the square pyramid. Another way to describe the structure of the square pyramid is in terms of the angle between the apical sulfur ligand, S_a, and a basal sulfur or CO ligand, L_b. If the Fe atom were in the basal plane, the S_a–M–L_b angle would be 90°. In the $[FeS_3(CO)_2]^{6-}$ fragment considered here, however, this angle is about 106°, so that the ligands are folded back away from the apical sulfur ligand. This folding back can have rather dramatic effects on the energies of the metal-based orbitals in a square pyramid.[27] The d_{z^2} orbital in a square pyramid is of course stabilized by the absence of a sixth ligand, but when the basal ligands are folded back as described above, the d_{z^2} orbital is further stabilized by the weakening of the σ interactions between the basal ligands and the d_{z^2} orbital. In systems where there are no basal π-acceptor ligands these σ effects lead to splittings of the size shown in Figure 3 for the $[MoS_3(dtc)]^{2-}$ fragment in $Mo_2Co_2S_4(dtc)_2(CO)_2$. If the basal ligands are π acceptors, however, the d_{z^2} orbital is further stabilized, because this geometry now allows the ligand π-acceptor orbitals to begin to overlap and interact with the d_{z^2} orbital. It is this π effect that explains the stabilization of the Fe d_{z^2} orbitals in $Mo_2Fe_2S_4(Cp)_2(CO)_4$ and ultimately influences the cluster bonding. In this folded-back geometry, the energies of two of the t_{2g} orbitals (the d_{xz} and d_{yz} orbitals in our coordinate system) are also influenced by the basal π-acceptor ligands. The folding back, which leads to decreased overlap and thus decreased interaction between these orbitals and the π-acceptor ligands, results in a destabilization of the d_{xz} and d_{yz} orbitals. The destabilization of these orbitals, however (unlike the stabilization of the d_{z^2} orbital), does not have an effect on the number of metal–metal bonds in the cluster.

These results make it clear that when the coordination around any of the metals in the M_4S_4 core is square pyramidal, both the S_a–M–L_b angle and the nature of the basal-plane ligands influence the cluster bonding. It is more common than not that the S_a–M–L_b angle is greater that 90°, so assuming in general that the basal plane ligands are bent back, it is the nature of the basal plane ligands that is important to the metal–metal bonding in the cluster. When the square-pyramidal metal has basal π-acceptor ligands, the cluster will be able to accommodate more "metal" electrons (without breaking metal–metal bonds) than when the square-pyramidal metal has basal π-donor ligands. With π-acceptor ligands, nonbonding metal orbitals from the square-pyramidal fragments are sufficiently stabilized that they lie lower in energy than the cluster metal–metal-antibonding orbitals and are thus occupied before the antibonding orbitals. With π-donor ligands, these nonbonding orbitals lie at sufficiently high energies that antibonding orbitals will be occupied first.

Turning to the charge distribution in $Mo_2Fe_2S_4(Cp)_2(CO)_4$, we see that the calculated charges and overlap populations shown in Tables I and II for this cluster are similar to those for the other clusters considered here. The $Mo_2Fe_2S_4(Cp)_2(CO)_4$ and $Mo_2Ni_2S_4(Cp)_2(CO)_2$ cubes provide the opportunity to compare two clusters with the same Mo fragments, but only small differences are apparent. In $Mo_2Fe_2S_4(Cp)_2(CO)_4$ it is once again probably appropriate to assign formal oxidation states of Mo^{5+} and Fe^0, although in $Mo_2Fe_2S_4(Cp)_2(CO)_4$ Mo is slightly less positive and Fe slightly more positive than are Mo and Ni in $Mo_2Ni_2S_4(Cp)_2(CO)_2$. The more positive charge on Fe may result simply from the presence of two π-acceptor CO ligands per Fe versus one CO per Ni. Detailed analyses of very small changes are once again hampered by different configurations about the metals, and once again the similarities in charge distributions in these clusters are much more apparent than any marked differences.

It is interesting to consider how this cluster would be affected by reduction or oxidation. A reduction would of course add an

electron to an antibonding level, and some type of cluster distortion would be expected. Since the LUMO is antibonding between the Mo's and Fe's, we would expect these bonds to be most affected by reduction. On the other hand, oxidation should have little effect on the metal–metal bonding in the cluster, since oxidation would remove an electron from a nonbonding orbital. This is an interesting point, because it suggests that other clusters with lower electron counts might also have this structure. For example, a cluster where Mn replaced Fe in the $Mo_2Fe_2S_4$ core of $Mo_2Fe_2S_4(Cp)_2(CO)_4$ would have 16 instead of 18 "metal" electrons. Depending on the relative placement of the Mn nonbonding levels, the removal of two electrons could have different effects. If the Mn nonbonding d_{z^2} orbitals were sufficiently stabilized that they were lower in energy than all of the antibonding orbitals, the cluster could be completely metal–metal bonded, with six bonding and two nonbonding orbitals occupied and no occupied antibonding oribitals. On the other hand, if the Mn nonbonding d_{z^2} orbitals were not sufficiently stabilized, the cluster could have a structure similar to that of $Mo_2Fe_2S_4(Cp)_2(CO)_4$ with six bonding orbitals and one antibonding orbital occupied and two electrons occupying either one or two nonbonding orbitals.

Finally, it is informative to consider the possibility of occupying the sixth coordination site on the Fe's in $Mo_2Fe_2S_4(Cp)_2(CO)_4$. We saw above from the comparison of $Mo_2Co_2S_4(dtc)_2(CH_3CN)_2(CO)_2$ and $Mo_2CO_2S_4(dtc)_2(CO)_2$ that the electronic structure of the $Mo_2Co_2S_4$ cube is perturbed very little by the occupation of the sixth coordination site on Mo. An examination of the energy level diagram in Figure 5 suggests that this will not be the case for $Mo_2Fe_2S_4(Cp)_2(CO)_4$. Occupying the sixth coordination site on each Fe, thus converting the Fe's to octahedral coordination, would destabilize each of the d_{z^2} orbitals sufficiently that the four electrons occupying these nonbonding orbitals on the square-pyramidal Fe's would now occupy antibonding levels. As a result, a total of three antibonding levels would be occupied, and we would expect gross distortions from the regular cube structure. In fact, the cluster $Mo_2Fe_2S_4(CH_3Cp)_2(CO)_6$ (**2**), which

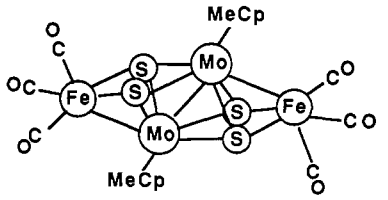

2

has an additional CO coordinated to each Fe, does exist.[11,32] It does not, however, have the familiar M_4S_4 cubane-type core. Instead, the four metals lies in a plane and are bridged by four μ_3-sulfido ligands. The structure of this cluster, which exhibits only three metal–metal bonds, can be viewed as a very distorted relative of the cube and is consistent with the orbital structure of $Mo_2Fe_2S_4(Cp)_2(CO)_4$. In contrast to the $Mo_2Co_2S_4$ cube, where the cube structure is independent of whether the Mo's are octahedral or square pyramidal, the cube structure of the $Mo_2Fe_2S_4$ core is thus destroyed by the presence of a sixth ligand coordinated to the Fe's. The difference results from the very important fact that in the $Mo_2Co_2S_4$ cube the change in coordination affects only unoccupied cluster orbitals. In the $Mo_2Fe_2S_4$ cube, the change in coordination affects occupied orbitals and thus has an impact on the cluster bonding.

(32) Cowans, B.; Noordik, J.; Rakowski DuBois, M. *Organometallics* **1983**, *2*, 931–932.

Conclusions

In summary, the results of calculations for several heterometallic cubane-type clusters illustrate how the electronic structure and, in particular, the formation of metal–metal bonds in the clusters are influenced by the ligand environment of each metal in the cluster. Metal–metal bonds are formed between t_{2g}-like metal orbitals, while e_g-like orbitals do not take part in the metal–metal bonding. (This is in contrast to the case of metal carbonyl clusters, where e_g-like orbitals are used to form metal–metal bonds and t_{2g}-like orbitals remain nonbonding between the metals.) The ligand environment (both the ligand geometry and the nature of the ligands) of each metal has a strong influence on the relative energies of these t_{2g}-like and e_g-like orbitals and thus has a strong influence on the energies of the bonding, antibonding, and nonbonding cluster orbitals. The position of the nonbonding orbitals determines how many "metal" electrons the cluster can accommodate without the loss of metal–metal bonds. Viewing the metal cluster orbitals in terms of metal "fragment" orbitals allows us to relate the metal–metal bonding in these seemingly different heterometallic clusters and to suggest possible new stable heterometallic clusters.

The charge distributions in the clusters are very similar and suggest that for all the clusters considered here it is probably appropriate to assign formal oxidation states of Mo^{5+} and M'^0 (M' = Fe, Co, Ni). The small values of the metal–metal overlap populations indicate that the direct metal–metal bonds are weak. Thus delocalized metal–sulfur–metal interactions rather than strong direct metal–metal bonds provide most of the "glue" holding together the $Mo_2M'_2S_4$ core. (Once again, this is in constrast to the case of metal carbonyl clusters, where stronger direct metal–metal bonds are generally responsible for holding together the core of the cluster.) The relative sizes of the metal–metal overlap populations indicate that the strength of the metal–metal bonds decreases in the order Mo–Mo > Mo–M' > M'–M'. Because of the very weak interactions between the 3d metals, the lowest energy metal–metal-antibonding orbital is antibonding between the 3d metals. As a result, the bond between the 3d metals is the first one affected by the occupation of an antibonding orbital.

By considering how the ligand environment of each metal ultimately influences the metal–metal bonding in the cluster, it is possible not only to systematically describe the metal–metal bonding in the heterometallic cubanes but also to relate the bonding picture developed here to the bonding in the numerous homometallic cubanes. This idea will be discussed in more detail in a future paper.

Acknowledgment. I am grateful to Drs. Ed Stiefel and Tom Halbert for many useful discussions.

Registry No. $Mo_2S_4(S_2CNEt_2)_2$, 67814-43-1; $Mo_2Co_2S_4(S_2CNEt_2)_2(CH_3CN)_2(CO)_2$, 97570-40-6; $Mo_2Ni_2S_4(C_5H_4Me)_2(CO)_2$, 105333-18-4; $Mo_2Fe_2S_4(C_5Me_5)_2(CO)_4$, 94619-63-3.